2020 SNMMI Highlights Lecture: Neuroscience

Julie Price, PhD, Professor of Radiology, Harvard Medical School, and Director, PET Pharmacokinetic Modeling, Athinoula A. Martinos Center for Biomedical Imaging, Massachusetts General Hospital, Boston, MA

From the Newsline Editor: The Highlights Lecture, presented at the closing session of each SNMMI Annual Meeting, was originated and presented for more than 30 years by Henry N. Wagner, Jr., MD. Beginning in 2010, the duties of summarizing selected significant presentations at the meeting were divided annually among 4 distinguished nuclear and molecular medicine subject matter experts. Each year Newsline publishes these lectures and selected images. The 2020 Highlights Lectures were delivered on July 14 as part of the SNMMI Virtual Annual Meeting. In this issue we feature the lecture by Julie Price, PhD, a professor of radiology at the Harvard Medical School and director of PET Pharmacokinetic Modeling in the Athinoula A. Martinos Center for Biomedical Imaging at the Massachusetts General Hospital (Boston, MA), who spoke on neuroscience highlights from the meeting. Note that in the following presentation summary, numerals in brackets represent abstract numbers as published in The Journal of Nuclear Medicine *(2020;61[suppl 1]).*

It is my pleasure to present the 2020 SNMMI Neuroscience Highlights Lecture. This year 8 oral sessions and 2 poster sessions focused on the neurosciences. A rough assessment indicated that these included presentations on neurodegeneration, including amyloid and tau deposition (~30%), synaptic function and metabolism (~25%), receptor/transporter imaging (~25%), and inflammation (~12%). The highlighted talks in this lecture will reflect this general distribution.

I would like first to congratulate Nicolaas Bohnen, MD, PhD, an internationally recognized researcher in Parkinson disease (PD) imaging, who received the 2020 Kuhl–Lassen Award from the SNMMI Brain Imaging Council. The award is given annually to recognize a scientist who has made outstanding contributions and whose research and service to the discipline of functional brain imaging is of the highest caliber. Examples of his innovative research were also seen in 2 presentations from his lab: "[18]F-FEOBV vesicular acetylcholine transporter network correlates of cognitive sub-domain functioning in PD" [357] and "Interaction of striatal dopaminergic and cholinergic activity in PD: A multimodal imaging study based on ^{11}C-DTBZ and ^{18}F-FEOBV PET combined with diffusion tensor imaging" [600].

Presentations were excellent in the Young Investigator Award Session for Brain Imaging. The participants once again showcased the extraordinary work being done in this area by our newest generation of scientists and clinicians. Although I will highlight a few of these presentations, I strongly encourage you to view the entire session, available on the SNMMI Virtual Meeting site.

Julie Price, PhD

Radiotracer Evaluation and Quantification

Neuroinflammatory changes, characterized by reactive astrocytes and activated microglia, contribute to neurodegeneration throughout the course of Alzheimer disease (AD). Reactive astrocytes overexpress monoamine oxidase-B (MAO-B) in the outer mitochondrial membrane. Okamura et al. from the Tohoku Medical and Pharmaceutical University/Tohoku University (Sendai, Japan), Commonwealth Scientific and Industrial Research Organisation (CSIRO; Melbourne, Australia), and Austin Health Melbourne (Australia) reported on "Evaluation of the novel ^{18}F-labeled PET tracer SMBT-1 for imaging astrogliosis in AD" [457]. Strong preclinical evaluation verified that ^{18}F-SMBT-1 bound reversibly to MAO-B with high affinity and selectivity, with significantly greater binding in AD brain. Regional concentrations were consistent with MAO-B concentration in human brain, as also evident in human PET imaging acquired 60–90 minutes postinjection (Fig. 1). In patients with AD, ^{18}F-SMBT-1 retention was significantly elevated in parahippocampal, fusiform, and inferior temporal gyri
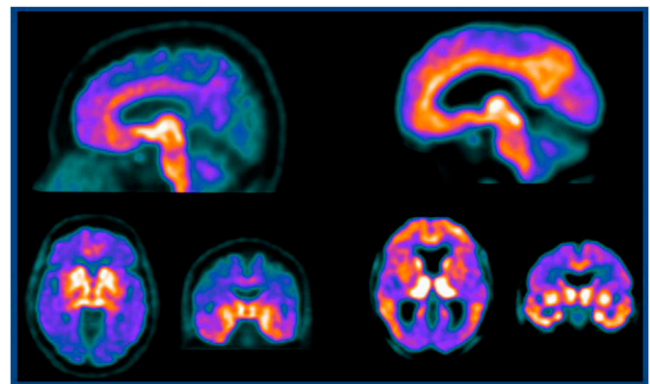

FIGURE 1. ^{18}F-SMBT-1 imaging of astrogliosis in Alzheimer disease (AD). Images acquired at 60–90 minutes postinjection in healthy controls (left 3 images) and individuals with AD (right 3 images). In AD, regional concentrations of monoamine oxidase-B (MAO-B) were significantly elevated in parahippocampal, fusiform, and inferior temporal gyri and overlapped with amyloid-β and tau deposition. ^{18}F-SMBT-1 showed high binding selectivity for MAO-B, highlighting the potential for clinical assessment of astrogliosis.
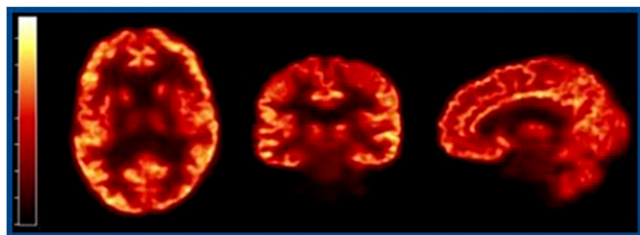
FIGURE 2. First-in-human study of ^{18}F-SynVesT-2. This novel SV2A radioligand showed favorable kinetics and test/retest reliability in comparison with ^{11}C-UCB-J and ^{18}F-SynVesT-1, with the potential for significantly reducing scan times and enabling new insights into abnormal synaptic density changes in neuropsychiatric disorders.

and overlapped with amyloid-β and tau deposition. ^{18}F-SMBT-1 binding was completely displaced after treatment with selegiline, indicating high binding selectivity for MAO-B and highlighting the potential for use of this novel radiotracer in clinical assessment of astrogliosis.

Cai et al. from Yale University School of Medicine/Yale University (New Haven, CT) reported on a "First-in-human study of ^{18}F-SynVesT-2, a novel SV2A [synaptic vesical glycoprotein-2] radioligand with fast kinetics and high specific binding signals" [462]. This radiotracer was found to have favorable properties compared to ^{11}C-UCB-J and ^{18}F-SynVesT-1, exhibiting faster kinetics and high test/retest reliability, although the volume of distribution and binding potential were generally lower. ^{18}F-SynVesT-2 provides promise for short scan times, with a V_T at 30 minutes within 10% of that at 120 minutes (Fig. 2). More readily available ^{18}F-labeled SV2A imaging probes can provide insights into abnormal synaptic density changes associated with many neuropsychiatric diseases. The authors noted that the pharmacokinetic characteristics of this tracer could potentially negate the need for arterial blood sampling, decreasing the burden on this patient population and facilitating large-scale clinical trials.

Moving on to a focus on quantification, Brumberg et al. from the Karolinska Institutet (Stockholm, Sweden), University Hospital Würzburg (Germany), and AstraZeneca (Stockholm, Sweden) reported that "Early peak equilibrium is superior to late pseudo-equilibrium for simplified quantification of ^{18}F-FE-PE2I PET" [455]. They looked at the cross-sectional, test–retest, and 2-year longitudinal performance of this dopamine transporter radioligand, based on dynamic data acquired in PD patients and controls to assess the performance of simplified binding ratios (SBRs) at early (15–45 minutes) peak equilibrium and late (51–81 minutes) pseudo-equilibrium in caudate and putamen. Early peak SBRs provided similar results to late scan SBRs for PD/control discrimination and annual percent change, although early SBR metrics were more favorable and similar to the more quantitative reference tissue binding potential results. Early SBR yielded better test–retest reliability, such that overall percent change was comparable for early and late SBR. Decline in binding was significant only for early SBR, indicating that this is preferable as a marker for disease progression and severity in ^{18}F-FE-PE2I imaging.

Neuroimmune Response

Zhang et al. from the General Hospital of Ningxia Medical University (Yinchuan, China) and the Turku PET Centre (Finland) reported on "In vivo PET imaging of neuroinflammation response after intravenous transplantation of olfactory ensheathing cells [OECs] in a hemisection spinal cord injury rat model" [213]. In a previous study the group had shown that neuroinflammation, a prominent neuropathologic feature of spinal cord injury, could be decreased by this method of intravenous cell transplantation. In the study reported at this meeting, they used F-^{18}F-DPA, a translocator protein (TSPO) radiotracer, for PET/CT, as well as spinal cord autoradiography, to show that inflammation was extensively increased without treatment but significantly decreased 7 days after OEC transplantation
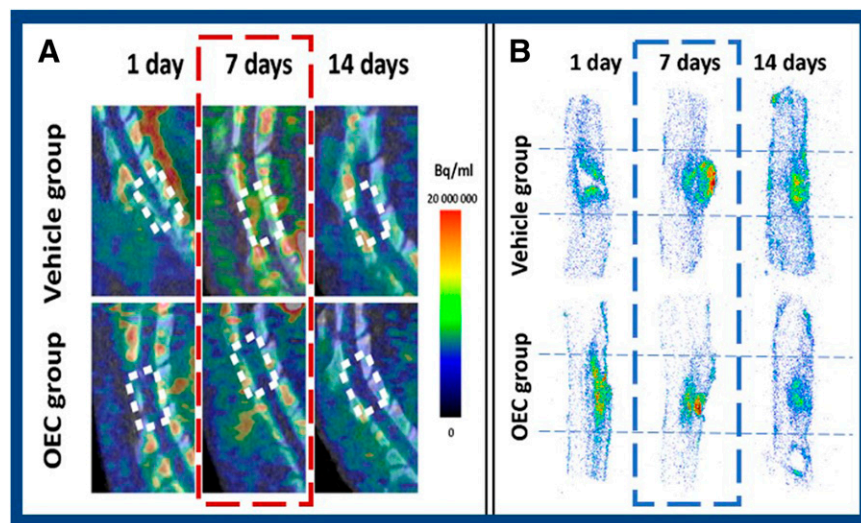

FIGURE 3. In vivo PET imaging of neuroinflammation response after intravenous transplantation of olfactory ensheathing cells (OECs) in a hemisection spinal cord injury rat model. (A) ^{18}F-DPA PET imaging (top row, vehicle only; bottom row, after OEC transplantation) at (left to right) 1, 7, and 14 days showed extensively increased inflammation without treatment that was significantly decreased 7 days after OEC transplantation. (B) Corresponding ^{18}F-DPA autoradiography (as well as histopathology, not pictured) confirmed these findings. Intravenous transplantation of OECs may mediate activated microglia to inhibit neuroinflammation after spinal cord injury.
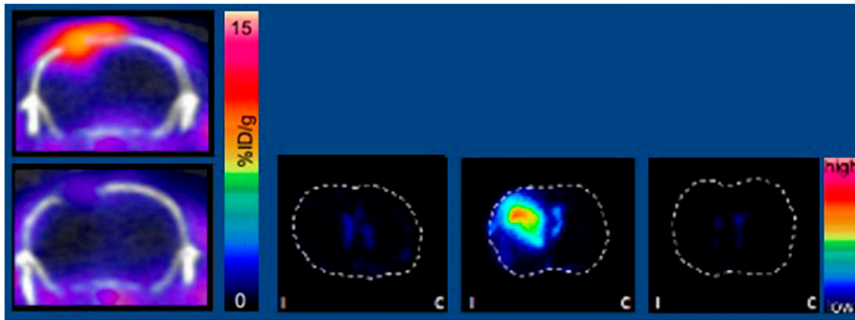
FIGURE 4. $_{64}$Cu-TREM1-monoclonal antibody (mAb) PET visualization of innate central nervous system immune activation in a mouse model of Parkinson disease. Left: Visualization of early innate immune activation at day 7 after injection of dopaminergic neurotoxin 6-hydroxydopamine (6-OHDA; top), compared with saline carrier alone (bottom). Right: $_{64}$Cu-TREM1-mAb ex vivo autoradiography at 7 days in (left to right) saline injected mouse, 6-OHDA injected mouse, and after TREM-1 knockout.

(Fig. 3), as confirmed also by Iba-1 and TSPO immunostaining. They concluded that intravenous transplantation of OECs can mediate activated microglia to inhibit neuroinflammation after spinal cord injury.

PD is strongly associated with aberrant adaptive and innate immune system responses, including microglial activation and infiltration of peripheral myeloid cells into the central nervous system. Katherine Lucot, PhD, and colleagues from Stanford University (CA), in work that was awarded a third-place Young Investigator Award from the Brain Imaging Council, reported on "Visualizing innate immune activation in a mouse model of PD using a highly specific TREM1-PET tracer" [16]. They evaluated the utility of this ^{64}Cu-labeled TREM1-monoclonal antibody (mAb) agent for detecting innate central nervous system immune activation in a widely used PD animal model based on intrastriatal injection of the dopaminergic neurotoxin 6-hydroxydopamine (6-OHDA). Elevated binding of the TREM1-PET tracer was observed in the striatum of 6-OHDA–treated mice at 7 days postsurgery by PET and autoradiography, but not at 14 days (Fig. 4). Immunostaining

showed PET and autoradiography signals to correspond with activated myeloid cells (i.e., tyrosine hydroxylase and CD68). The authors concluded that elevated levels of activated myeloid cells could be detected in this PD mouse model using the ^{64}Cu-TREM1-mAb and that TREM1-PET is a promising specific approach for visualizing early innate immune activation.

PET imaging of the 18-kDA TSPO may provide a useful biomarker that is sensitive to dynamic changes in the immune system. Hillmer et al. from the Yale University School of Medicine/Yale University (New Haven, CT) and the Veterans Affairs Connecticut Healthcare System (West Haven) reported on "Preliminary evidence for ^{11}C-PBR28 sensitivity to alcohol challenge in human brain" [458]. These authors investigated the sensitivity of ^{11}C-PBR28 TSPO PET imaging to an oral alcohol challenge targeting peak blood alcohol concentrations of 80 mg/dL (common legal limit). A baseline scan was acquired on the morning before the alcohol challenge, which then began about 2.5 hours before the 90-minute post-alcohol scan. The average post-alcohol ^{11}C-PBR28 V_T values across 6 participants were
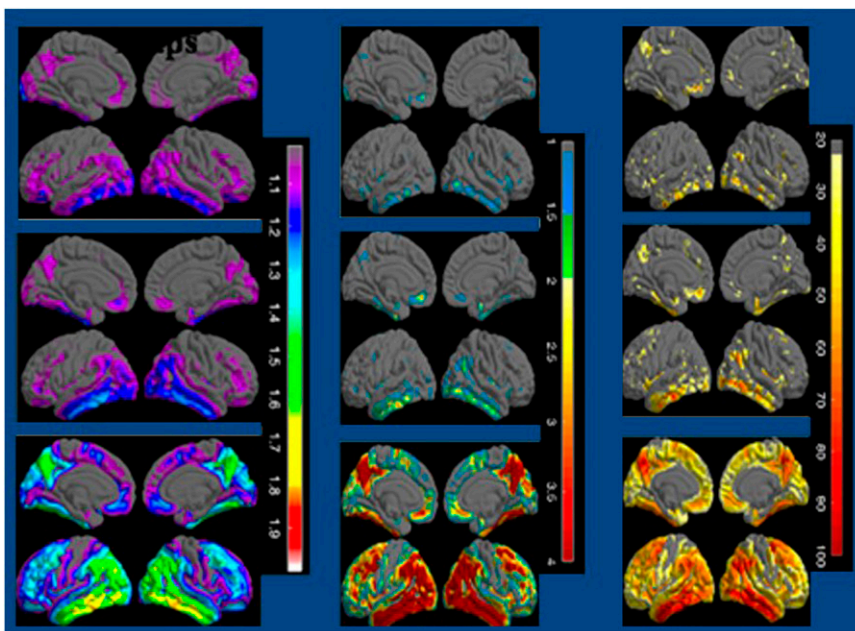

FIGURE 5. ^{18}F-flortaucipir retention grouped according to autopsy-confirmed neurofibrillary tangles (NFTs). Groupwise surface mapping analyses showing (left to right) SUV ratios, Z scores relative to young healthy controls, and percentage of subjects with Z scores >2 in individuals assigned on the basis of NFTs to groups (top to bottom in rows of 2): Braak I/II ($n = 7$), Braak III/IV ($n = 15$), and Braak V/VI ($n = 38$). Tracer retention patterns at a group level, then, agreed with the staging scheme proposed by Braak and Braak.
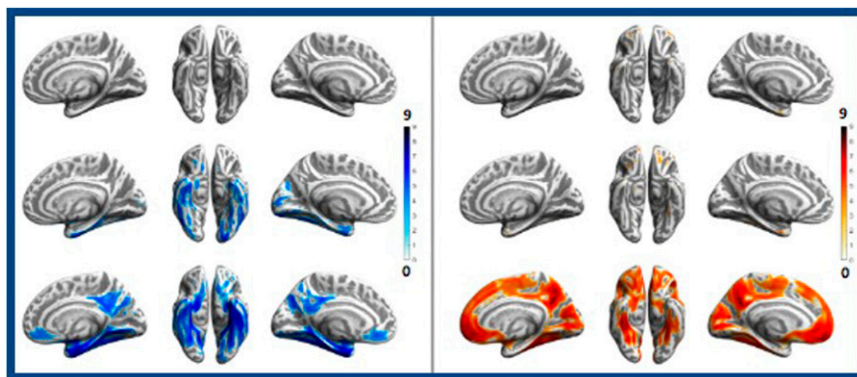
FIGURE 6. Resistance to tau and amyloid pathology in super-aging. Tau and amyloid distribution patterns in different cognitive aging trajectories for (rows top to bottom): super-agers, normal agers, and individuals with mild cognitive impairment (MCI). Left block: tau pathology (in blue). Right block: amyloid pathology (in orange). Results indicated that super-aging appears to be associated with resistance to tau and amyloid pathology, which likely permits maintenance of cognitive performance despite advanced age. Differences between normal aging and MCI appear to be driven by amyloid burden levels. These data support the need for research into factors underlying resistance to tau and amyloid pathology, which could lead to development of novel treatment concepts. This was selected as the Image of the Year during the SNMMI Annual Meeting in July 2020.

about 21% higher than baseline levels in cortical and subcortical areas (frontal cortex, hippocampus, striatum, and cerebellum). The data provide preliminary evidence that PBR28 PET can measure the acute neuroimmune response to alcohol and show promise for future studies of problematic alcohol use.

Amyloid, Tau, and Neurodegeneration

Another participant from the Young Investigator Award session, Kotari et al. from Avid Radiopharmaceuticals (Philadelphia, PA), reported on "Visualization of flortaucipir retention in subjects grouped according to their autopsy-confirmed neurofibrillary tangle scores" [19]. These researchers retrospectively analyzed a 60-subject flortaucipir tau PET dataset from a prior phase III autopsy study for which image interpretation predicted autopsy-confirmed neurofibrillary tangle scores at the later B3 stage (equivalent to Braak V/VI) and showed improved sensitivity to an earlier (B2) pathology stage was gained using an early tau volume-of-interest. The current work applied groupwise surface map analysis for visualization of antemortem flortaucipir retention based on neurofibrillary tangle scores and found that tracer retention patterns at a group level agreed with the staging scheme proposed by Braak and Braak (Fig. 5).

The phenomenon of cognitive "super-aging," with some individuals performing significantly above the norm despite being quite advanced in age, suggests specific resistance mechanisms against brain aging processes and/or neurodegeneration and is receiving increased research attention. Merle Hoenig, PhD, first-place Young Investigator Award winner, and colleagues from University Hospital Cologne, the Brain Research Center Jülich, and the German Center for Neurodegenerative Diseases (Bonn and Cologne; all in Germany) reported that "Resistance to tau and amyloid pathology facilitates super-aging" [20]. They compared the intracerebral amyloid and tau burdens in age- and education-matched groups of >80-year-old super-agers, normal-agers, and patients with mild cognitive impairment (MCI) using data from the Alzheimer's Disease Neuroimaging Initiative relative to younger (mean age, 63 years) cognitively normal and amyloid-negative controls. Looking across several regions and on a voxel-level basis, the investigators nicely demonstrated that super-aging appears to be associated with resistance to tau (flortaucipir) and amyloid (florbetapir) pathology, which likely permits maintenance of cognitive performance despite advanced age. Differences between normal aging and MCI, however, appear to be driven by amyloid burden levels. Results from this study, providing evidence of a conceptual continuum progressing from successful aging, to age-related tau tangle aggregation, to pathological aging, were named as the prestigious SNMMI Image of the Year (Fig. 6). These results provide additional data supporting research into factors
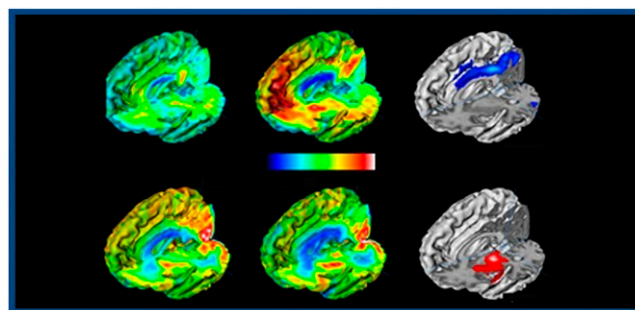

FIGURE 7. Regional associations between amyloid and glucose metabolism during Alzheimer disease (AD) progression in Down syndrome (DS). ^{11}C-Pittsburgh compound B Aβ (top row) and ^{18}F-FDG (bottom row) PET imaging (0-3 SUVR) in (left) a cognitively stable individual (38 years old) with DS; (middle) confirmed mild cognitive impairment/AD in a 55-year-old with DS; and (right) t-score maps of significant voxel clusters showing patterns of hypometabolism (top) and hypermetabolism (bottom) with elevated Aβ. Images are overlaid on MRI surface projections of healthy DS brain. ^{18}F-FDG hypometabolism with elevated amyloid was most prominent in the parietal cortex, precuneus, and posterior cingulate, indicating that ^{18}F-FDG PET can provide valuable information on neurodegeneration status for DS. A unique pattern of ^{18}F-FDG hypermetabolism in the putamen of the striatum was also identified in DS.
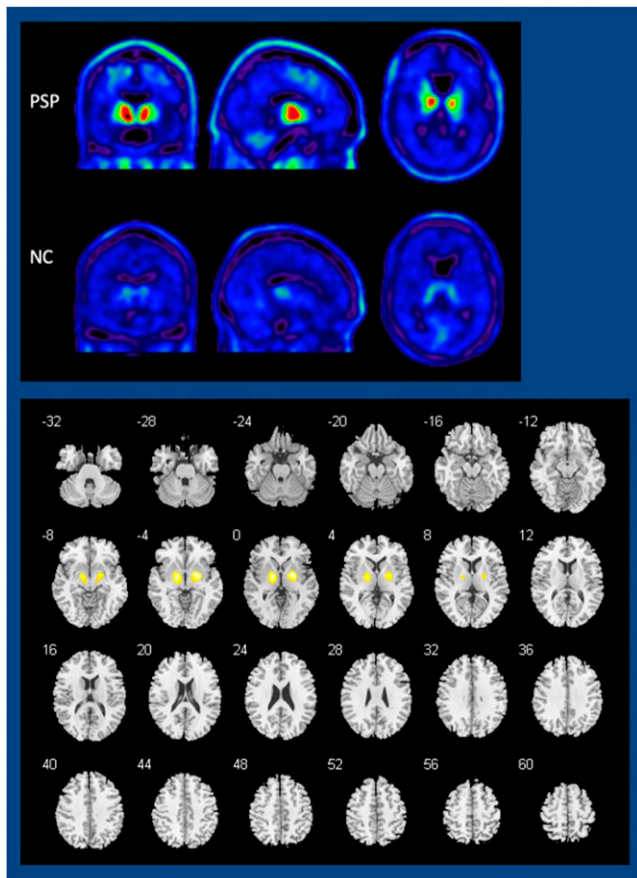
FIGURE 8. ^{18}F-APN-1607 in progressive supranuclear palsy (PSP). Top block: Examples of superimposed ^{18}F-APN-1607 PET and anatomic MR images in a patient with PSP (top) and a normal control (NC) subject. Bottom block: Voxel-wise differences of ^{18}F-APN-1607 uptake between PSP and NC groups. Regional ^{18}F-APN-1607 SUV ratio load was significantly elevated in PSP patients in several subcortical areas compared with controls, consistent with observations at the voxel level, which suggests potential for future in vivo investigations into relationships between tauopathies and clinical assessments in PSP.

underlying resistance to tau and amyloid pathology, which could lead to development of novel treatment concepts.

Second-place Young Investigator Awardee Matthew Zammit, MS, and colleagues from the University of Wisconsin-Madison, the University of Pittsburgh (PA), the University of Cambridge (UK), and Washington University in St. Louis (MO) representing the Alzheimer's Biomarkers Consortium–Down Syndrome, reported on "Regional associations between amyloid and glucose metabolism during the progression of AD in Down syndrome" [21]. They assessed the utility of ^{18}F-FDG PET in classifying neurodegeneration within the A/T(N) framework in 81 adults (ages, 38.9 ± 8.3 years) with Down syndrome who underwent both ^{11}C-Pittsburgh compound B and ^{18}F-FDG PET imaging. The researchers found that ^{18}F-FDG hypometabolism with elevated amyloid was most prominent in the parietal cortex, precuneus, and posterior cingulate (Fig. 7). Regional glucose metabolism changes appear to be similar in

Down syndrome and sporadic AD, indicating that ^{18}F-FDG can provide valuable information on neurodegeneration status within the A/T(N) framework for Down syndrome. A unique pattern of ^{18}F-FDG hypermetabolism in the putamen of the striatum was identified, possibly in response to an abundance of diffuse amyloid in this region, suggesting that the putamen is spared from metabolic reductions associated with neurodegeneration in these individuals.

Li et al. from Huashan Hospital/Fudan University (Shanghai, China) reported on "Binding characteristics of the new-generation tau PET tracer ^{18}F-APN-1607 in progressive supranuclear palsy (PSP)" [461]. They explored the utility of this radioligand for assessing characteristic distributions of tau pathologies and associations with clinical symptoms in patients with PSP, a 4-repeat tauopathy with tau inclusions in brainstem and subcortical neurons. Findings showed that the regional ^{18}F-APN-1607 SUV ratio (SUVR) load was significantly elevated in PSP patients in several subcortical areas compared with controls, consistent with observations at the voxel level (Fig. 8). The PSPRS—eye clinical rating score was found to be significantly correlated with the putamen SUVR in individuals with PSP. These results are promising for future in vivo studies of relationships between tauopathies and clinical assessments in PSP.

Rowe et al. from Austin Health Melbourne, the University of Melbourne, and CSIRO Melbourne (all in Australia) reported on "Tau accumulation over 1 year measured with F-18 MK6240 PET" [285]. This is a second-generation tau
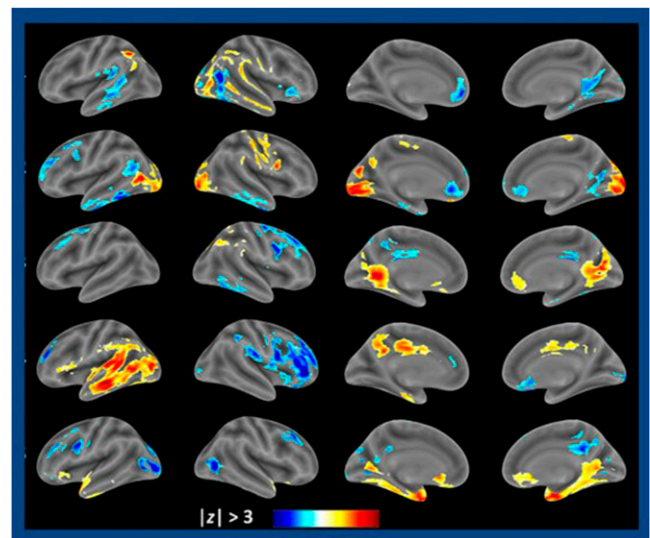

FIGURE 9. Independent component analysis (ICA) of SV2A ^{11}C-UCB-J-PET in Alzheimer disease (AD). Independent components 1–5 (top to bottom) in participants with AD and mild cognitive impairment (MCI) were found to have altered contributions (weights) to synaptic density patterns compared to cognitively normal individuals, and these were significantly different for AD participants. Spatial patterns for individuals in the MCI + AD groups correlated with cognitive assessments for independent component group 4 (left midtemporal/occipital lobe and cingulate cortex). Such assessments have the potential to monitor the dynamics of neurodegeneration severity longitudinally.

tracer with high target-to-background binding and negligible choroid plexus uptake, a phenomenon that complicates tau quantification for other tau radioligands. The researchers looked at 1-year progression and regional rates of tracer accumulation in cognitively normal participants and those with MCI and AD. For amyloid-negative individuals, no change in tau SUVR was noted after 1 year, but the rate of change was found to be proportional to baseline tau level and diagnosis. For amyloid-positive individuals, rates of change in tau SUVR ranged from +1.6%/year in the cognitively normal group to 4.1%/year in MCI and +6.7%/year in individuals with AD—larger changes than reported previously with flortaucipir imaging. Further longitudinal study is needed to better understand the relationships between ^{18}F-MK6240 SUVR change, age, and baseline SUVR.

Network Analyses in Neurodegenerative Disorders

Regional synaptic loss is a biomarker for a variety of neurodegenerative and neuropsychiatric disorders, and synaptic density PET imaging of synaptic vesicle glycoprotein 2A (SV2A) has the potential for utility in the study, diagnosis, and staging of diseases, as well as evaluation of therapeutic effects. Fang et al. from Yale University/Yale New Haven Hospital (CT) reported that "Independent component analysis (ICA) of synaptic density of ^{11}C-UCB-J-PET in AD identifies networks correlated with cognitive impairment" [343]. The researchers applied ICA to ^{11}C-UCB-J PET data acquired in cognitively normal, MCI, and AD subjects to identify brain networks associated with cognitive deficits in AD. The investigators found that MCI and AD subjects had altered contribution (loading weights) to synaptic density patterns compared to cognitively normal individuals that was significantly different for AD participants (Fig. 9). Spatial patterns for the MCI + AD groups correlated with cognitive assessments, with significant relationships between IC4 weights in the left midtemporal/occipital lobe and cingulate cortex and Cognitive Dementia Rating Scale (CDR), Logical Memory II, and Mini-Mental State Examination (MMSE) scores. The ICA-based network analyses have the potential to monitor the dynamics of neurodegeneration severity (i.e., disease progression) longitudinally, as well as to monitor treatment effects.

With the increasing use of subthalamic nucleus (STN) deep brain stimulation (DBS) in the treatment of PD, objective/quantitative criteria are needed to assess therapeutic outcomes. Ge et al. from Huashan Hospital/Fudan University (Shanghai, China) and the University of Bern (Switzerland) reported on "Metabolic network as an objective biomarker in monitoring DBS for PD: A longitudinal study" [341]. These authors investigated the utility of the ^{18}F-FDG PD-related metabolic network pattern (PDRP) for monitoring of STN DBS in PD patients over time. The PDRP is characterized by relative metabolic increases in putamen, pallidum, caudate, thalamus, cerebellum, pons, and olfactory regions and metabolic decreases in posterior parietal-occipital

cortices. Both the PDRP score and clinical Unified PD Rating Scale were found to decrease (improve) at 3 months after STN DBS but then return to baseline levels at 12 months after treatment. Graphical network analysis of PDRP expression indicated increased connections 3 months after STN DBS and a return at 12 months posttreatment (Fig. 10). Preliminary results from the study indicate the potential of PDRP expression as a complementary objective biomarker for assessment and monitoring of STN DBS in PD over time.

The cholinergic system plays an important role in the cognitive impairment syndrome of PD. Previous acetylcholinesterase PET imaging studies have found memory, attention, and executive function correlates of global cortical cholinergic losses in PD. van der Zee et al. from the University of Groningen (The Netherlands) and the University of Michigan (Ann Arbor) reported on "^{18}F-FEOBV vesicular acetylcholine transporter network correlates of cognitive sub-domain functioning in PD" [337]. These authors looked at relationships between cognitive domain functioning and regional cerebral cholinergic innervation using ^{18}F-FEOBV PET in a population of 86 non-demented PD patients (ages, 67.8 ± 7.6 years; motor disease duration, 5.8 ± 4.6 years). Voxel-based analyses showed specific but partially overlapping topographic
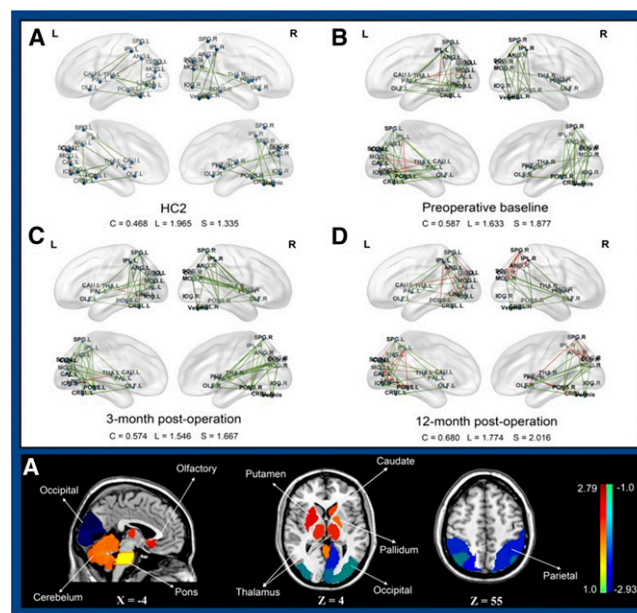

FIGURE 10. ^{18}F-FDG PD-related metabolic network patterns for monitoring subthalamic nucleus (STN) deep brain stimulation (DBS) in patients with Parkinson disease (PD). Top block: Graphical network analyses in (A) healthy controls; (B) PD patients at baseline; (C) PD patients at 3-months post-STN DBS; and (D) PD patients at 12-months post-STN DBS. The network analysis indicated increased connections 3 months after STN DBS and a return at 12 months posttreatment. Bottom row: ^{18}F-FDG PDRP imaging pattern. PET-assessed PDRP expression has potential as a complementary objective biomarker for assessment and monitoring of STN DBS in PD over time.
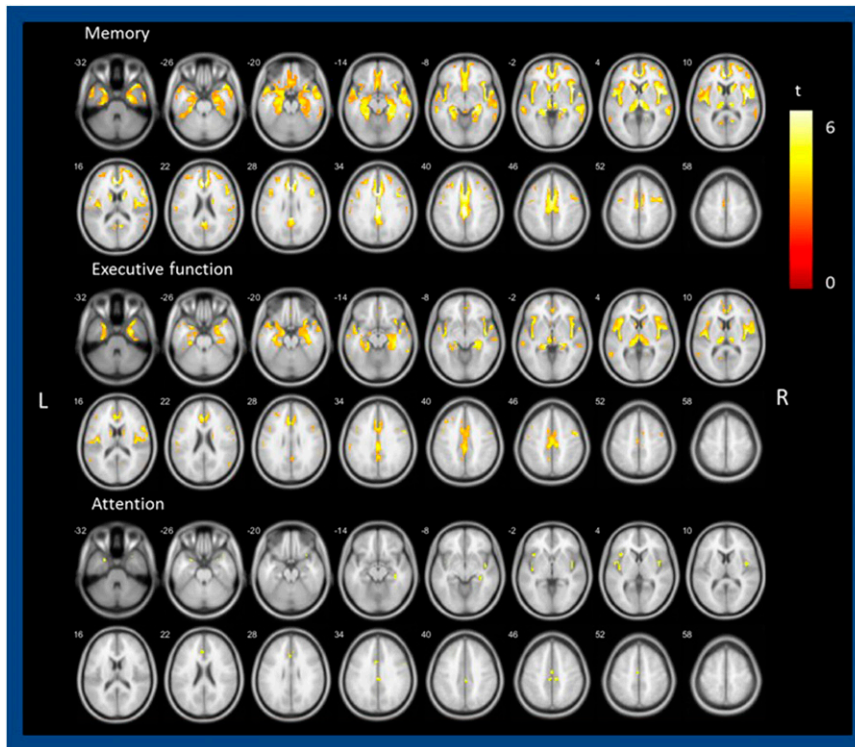
FIGURE 11. ^{18}F-FEOBV vesicular acetylcholine transporter network correlates of cognitive sub-domain functioning in Parkinson disease (PD). Voxel-based analysis of images acquired in nondemented PD patients showed a partial topographic overlap of cholinergic system correlates assessed with ^{18}F-FEOBV across different cognitive domains (top 2 rows, memory; middle 2 rows, executive function; bottom 2 rows, attention), suggesting a shared cholinergic network function subserving overall cognitive functioning. Involvement of the visual thalamus also suggested a cholinergic role in visual processing in modulation of these 3 cognitive functions in PD.

cholinergic profiles for each of the cognitive domains (Fig. 11). This was thought to reflect a shared cholinergic network function subserving overall cognitive functioning. One striking finding was the involvement of the visual thalamus across multiple domains, suggesting a cholinergic role in visual processing in the modulation of memory, attention, and executive functioning.

Multimodal Imaging and Dopaminergic and Cholinergic Interactions

Huntington disease (HD) is an inherited disorder that involves degeneration of the basal ganglia. Pridopidine, with a pharmacologic effect mainly mediated via sigma-1 receptor (S1R) interaction, is under development as a drug to reduce motor impairment in HD. Barthel et al. from University Hospital Leipzig (Germany), ABX-CRO Advanced Pharmaceutical Services (Dresden, Germany), Teva Branded Pharmaceutical Products (Frazer, PA), and Prilenia Therapeutics Development (Herzliya, Israel) reported on "Multiple brain effects of pridopidine in HD patients and healthy volunteers: A simultaneous sigma-1 receptor PET/MRI study' [336]. These researchers applied ^{18}F-fluspidine (S1R imaging agent) and simultaneous PET/MR imaging to investigate the pridopidine effect on neurotransmission, brain perfusion, metabolism, and functional connectivity. In 7 healthy volunteers, 90 mg of pridopidine occupied about 90% of S1Rs, decreased regional cerebral blood flow in temporal and cerebellar areas, decreased myo-inositol/N-acetylaspartylglutamate
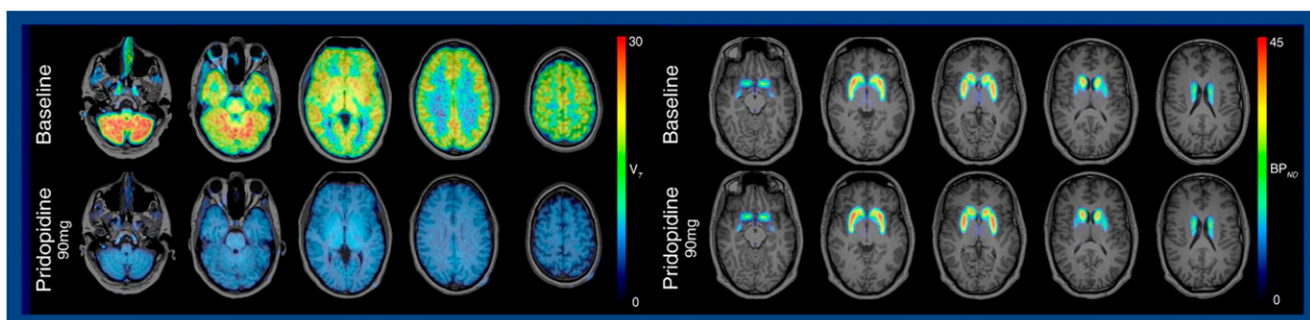

FIGURE 12. ^{18}F-fluspidine and ^{18}F-fallypride PET and pridopidine mechanism of action. Left block: Baseline (top) and post-pridopidine (90 mg) (bottom) ^{18}F-fluspidine PET in a healthy volunteer showing full S1R occupancy (~90%). Right block: Baseline (top) and post-pridopidine (90 mg) (bottom) ^{18}F-fallypride PET in a healthy volunteer showing minimal dopamine-2/dopamine-3 receptor occupancy at clinically relevant doses of pridopidine. These results support use of pridopidine to achieve full selective S1R targeting in future Huntington disease and amyotrophic lateral sclerosis clinical trials.
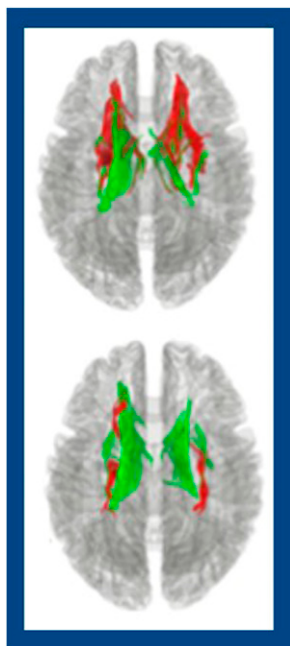
FIGURE 13. ^{11}C-DTBZ and ^{18}F-FEOBV PET combined with diffusion tensor imaging to elucidate interaction of striatal dopaminergic and cholinergic activity in Parkinson disease phenotypes. Top: Tremor dominant phenotype. Bottom: Mobility impairment phenotypes. Image analysis showed a differential relationship between tracts associated with dopaminergic (red) and cholinergic (green) nerve terminals, suggesting that the PD phenotype may be driven, in part, by changes in the balance interaction between striatal dopaminergic and cholinergic systems.

(NAA) ratios in white matter, and increased connectivity for some within the basal ganglia network and default mode network. The authors concluded that pridopidine in a clinically tested dose shows full S1R occupancy in HD patients and HVs, which is associated with multiple effects on brain perfusion, metabolism, and functional connectivity. This is an example of the wealth of data and information that can be acquired from multimodality imaging in neurodegeneration that can improve understanding of drug effects in the brain.

Meyer et al. from the University of Leipzig (Germany), Guide Pharmaceutical Consulting (Millstone Township, NJ), Teva Branded Pharmaceutical Products R&D (Malvern and Frazer, PA), ABX-CRO Advanced Pharmaceutical Services (Dresden, Germany), Helmholtz-Zentrum Dresden-Rossendorf (Leipzig, Germany), and Prilenia Therapeutics Development (Herzliya, Israel) reported on "High S1R but minimal dopamine-2/dopamine-3 receptor (D2/D3R) occupancy at clinically relevant doses of pridopidine in healthy volunteers and HD patients investigated by using (S)-(-)- ^{18}F-fluspidine and ^{18}F-fallypride PET" [338]. Their aim was to clarify pridopidine's mechanism of action in the human brain in vivo, where it was originally thought to act as a dopamine stabilizer. Their results revealed that a single oral dose of 90 mg pridopidine that resulted in ~90% S1R occupancy was accompanied by minimal (~3%) D2/D3R occupancy in the ^{18}F-fallypride study (Fig. 12). The authors concluded that the PET findings support use of pridopidine 45 mg doses twice daily to achieve full selective S1R targeting in future HD and amyotrophic lateral sclerosis clinical trials.

I will end with a collaborative study presented from researchers at Dr. Bohnen's lab. Sanchez-Catasus et al. from University Medical Center Groningen (The Netherlands), the University of Michigan Health System (Ann Arbor), KU Leuven (Belgium), and the Veterans Administration Ann Arbor Healthcare System (MI) reported on "Interaction of striatal dopaminergic and cholinergic activity in PD: A multimodal imaging study based on ^{11}C-DTBZ and ^{18}F-FEOBV PET combined with diffusion tensor imaging [DTI]" [600]. Their goal was to examine the relationship between striatal dopaminergic and cholinergic nerve terminal integrity (using ^{11}C-DTBZ and ^{18}F-FEOBV PET, respectively) and microstructural integrity of associated tracts (using DTI), and to explore resulting associations with the PD phenotype. The multimodal analyses provided evidence of a relationship between neurotransmitter nerve terminal integrity and axonal integrity (Fig. 13). Analysis of clinical phenotypes (e.g., tremor versus gait impairment) showed a differential relationship between tracts associated with dopaminergic and cholinergic nerve terminals, suggesting that PD phenotype may be driven, in part, by changes in the balance interaction between striatal dopaminergic and cholinergic systems.

Summary

I want to thank all the colleagues who sent slides for this lecture, and regret that time constraints did not allow me to show the broadest range of the extraordinary presentations from this meeting. I also want to fondly remember Henry N. Wagner, Jr., MD, who started and for many years delivered these annual lectures and to thank my SNMMI colleagues for including me in this new honor.